Kinetics of domain growth in systems with local barriers

Kumela Tafa, Sanjay Puri, and Deepak Kumar
School of Physical Sciences, Jawaharlal Nehru University, New Delhi, 110067, India
(Received 19 October 2000; published 29 March 2001)

We study domain growth in spin-1 lattice models having nonconserved spin-flip kinetics with local barriers. Our primary motivation is to model the relaxational behavior of physical systems in which molecular motion is impeded by local kinetic barriers. The kinetic constraint is such that a spin from an up (down) state can flip to a down (up) state only via the zero state, which has a higher energy. We examine how the usual curvature-driven domain growth is affected by these local barriers, and whether the single-spin barriers have a collective effect. This paper presents comprehensive numerical results for phase ordering dynamics in this model using Monte Carlo simulations. We demonstrate dynamical scaling for domain-size distribution functions and spatial correlation functions. We also present results for the time dependence of characteristic length scales and autocorrelation functions. The length-scale behavior is interpreted in terms of the random walk of steps on domain boundaries. Furthermore, we present a simple stochastic model to derive an analytic expression for the autocorrelation function, which exhibits a stretched-exponential behavior over an extended regime—in agreement with our numerical simulations.

DOI: 10.1103/PhysRevE.63.046115 PACS number(s): 64.60.−i

I. INTRODUCTION

There has been much interest in the temporal behavior of systems approaching equilibrium. Systems that have been quenched from a disordered phase to an ordered phase do not order instantaneously. Typically, the length scale of ordered regions grows with time as the different ordered phases compete to select an equilibrium state. The process whereby the system orders is referred to as ''phase ordering'' (or ''domain growth'' or ''coarsening''), and has now been studied extensively [1]. Perhaps the most relevant feature of phase ordering systems is that the time-dependent evolution subsequent to the quench usually exhibits a dynamical-scaling property [2,1]. Thus, the spatial correlation function $C(\vec{r},t)=\langle s(\vec{R},t)s(\vec{R}+\vec{r},t)\rangle$, where $s(\vec{r},t)$ is the appropriate order parameter (OP) at point $\vec{r}$ and time t after the quench, has the scaling form

$$C(\vec{r},t)=g\left(\frac{r}{L(t)}\right). \tag{1}$$

In physical terms, Eq. (1) reflects the fact that the morphology of the coarsening system, described by $g(x)$, is unchanged in time, but the scale of the morphology grows as $L(t)$. For pure and isotropic systems with a scalar OP, the growth of $L(t)$ depends on whether or not the OP is conserved by the system dynamics. For the case with nonconserved OP (NCOP), we have $L(t)\sim t^{1/2}$, which is referred to as the Allen-Cahn (AC) growth law. On the other hand, for the case with conserved OP (COP) and no hydrodynamic effects, we have $L(t)\sim t^{1/3}$, referred to as the Lifshitz-Slyozov growth law [1]. For randomly disordered systems that contain quenched impurities, the domain walls can be trapped and the growth of $L(t)$ becomes much slower, often exhibiting logarithmic time dependencies [3–5]. Recent interest has also focused upon logarithmically slow dynamics in systems without quenched disorder. An interesting work in this context is due to Shore *et al.* [6], who formulated arguments for slow domain growth in Ising models with competing interactions but no quenched disorder.

An alternative tool to characterize nonequilibrium (or equilibrium) systems is the autocorrelation function:

$$\Phi(t_0,t)=\langle s(\vec{r},t_0)s(\vec{r},t_0+t)\rangle-\langle s(\vec{r},t_0)\rangle\langle s(\vec{r},t_0+t)\rangle, \tag{2}$$

which explicitly depends on both times (t_0 and t) in the case of nonequilibrium systems. This quantity has been extensively studied in the context of glassy dynamics, where it is known to exhibit a stretched-exponential form [7–11]. Much effort has focused on understanding this slow dynamics, particularly in the context of systems without quenched disorder, e.g., structural glasses. Some analytical studies have also argued for similar stretched-exponential behavior of $\Phi(t_0,t)$ in equilibrium fluctuations of ordered ferromagnets [12,13]. However, these arguments have not been supported by the Monte Carlo (MC) simulations of Graham and Grant [14].

This paper focuses on the phase ordering dynamics of a special case of the spin-1 Blume-Emery-Griffiths (BEG) model [15]. The feature of the dynamics we study here is the introduction of local barriers to single spin-flip kinetics. The static properties of the BEG model have been extensively investigated [15–20], but there has been only limited study of its nonequilibrium properties. This paper presents detailed MC results for both spatial correlation and autocorrelation functions for the far-from-equilibrium dynamics of the BEG model.

Let us conclude this section by providing a broad overview of this paper. There are two primary goals of our paper. First, we wish to examine the manner in which local kinetic barriers affect growth kinetics and domain morphology, i.e., we investigate the validity of dynamical scaling in the context of a larger class of models. Second, we want to obtain an analytical understanding of autocorrelation functions in these models. This paper is organized as follows. Section II pro-

vides background material on domain growth, in the context of which our subsequent results will be interpreted. In Sec. III, we describe our model and provide a brief review of its static properties. In Sec. IV, we present and discuss our numerical results for (a) spatial correlation functions, (b) domain-size distribution functions, and (c) characteristic length scales. In Sec. V, we present our numerical results for the autocorrelation function and describe a simple stochastic model that mimics the evolution. Finally, Sec. VI concludes this paper with a brief summary of our results and some issues for future consideration.

II. CLASSES OF DOMAIN GROWTH IN SYSTEMS WITH NONCONSERVED ORDER PARAMETER

The phase ordering system evolves from an initial nonequilibrium configuration towards a final state by going through a number of intermediate configurations. The evolution of the system from one state to another can be understood in terms of paths in state space. The probability associated with a particular path is given by the usual statistical weight of intervening configurations, which is largely determined by the highest-energy configuration encountered along that path. At low temperatures, paths which encounter lowest-energy barriers will clearly dominate. At higher temperatures, the entropic factor arising from a multiplicity of paths should also be accounted for. Therefore, the evolution problem is equivalent to one of diffusion in a high-dimensional configuration space with a complex energy landscape. (Of course, we should stress that a better description would be in terms of the evolution of an ensemble of initial states to another ensemble of final states.)

Let as elucidate this point with a well-known example, i.e., the spin-1/2 ferromagnetic nearest-neighbor Ising model in dimension $d=2$ with zero-magnetic field. Let this system be quenched from a disordered initial state to a temperature T below its critical temperature T_c. Typically, the initial state has equal numbers of up and down spins, which are randomly distributed through the lattice. The system starts ordering locally, and soon develops a number of up and down domains, competing with each other to grow. As time goes on, the number of domains decreases due to growth in size of the remaining domains. To understand this coarsening, it is instructive to consider shrinking of a single square domain of side L. If we take the strength of the nearest-neighbor interaction to be J, the energy cost to flip a spin inside a domain is $8J$. On the boundary, this cost is $4J$, while it is 0 at the corners of the domain. Since a corner spin can be flipped without energy cost, the most probable path for domain shrinking begins with flipping of one of the corner spins, which creates two corners on the edges. This flip is followed by a random walk of the corner along an edge, each step of which has no energy cost. Thus, an edge of size L is eliminated in a time proportional to L^2. As a matter of fact, this time can be calculated quite accurately if one considers a one-dimensional random walk with probability p to jump right or left; and probability q of not jumping. The resultant expression for the first-passage probability of covering a distance L in t steps is a generalization of a formula due to Lagrange [21] :

$$P(L,t)=1-\frac{2}{2L-1}\sum_{k=0}^{L-1}\frac{\cos^2\phi_k}{\sin\phi_k}\{1-[q+2p\cos(2\phi_k)]^t\}, \tag{3}$$

where $\phi_k=\pi(2k+1)/(4L-2)$. The first-passage time (up to a prefactor) is obtained by setting $P(L,t)$ to a fixed value. This yields a $t\sim L^2$ behavior even at rather small values of L, as we have ascertained by explicit calculation.

In the general situation, the above considerations imply a coarsening length scale $L(t)\sim t^{1/2}$, providing an equivalent way of interpreting curvature-driven growth in the context of discrete lattice models [6]. Furthermore, since no energy barrier occurs on this path (i.e., corner performing random walk on an edge), such coarsening obviously occurs even at $T=0$.

An important step towards a broader understanding of domain growth laws is due to Lai *et al.* [22] (LMV), who provided a classification of domain-coarsening laws for nonconserved systems. They proposed four different classes of systems, determined by the dependence of the energy barrier to coarsening on the characteristic domain length. This classification is best understood by considering the equation for curvature-driven growth [1]:

$$\frac{dL(t)}{dt}=\frac{a(L,T)}{L(t)}, \tag{4}$$

where the function $a(L,T)$ is the diffusion coefficient, which depends on length scale and temperature, in general. Following the discussion of Shore *et al.* [6], the LMV classification can be stated in terms of the behavior of $a(L,T)$.

(a) *Class 1* systems are those for which $a(L,T)$ is independent of L and remains nonzero as $T\to 0$. In these systems, there exist relaxation paths that have no energy barrier and the nature of relaxation does not depend on the coarsening length scale. The Ising model discussed above clearly belongs to this class. In general, $L(t)\sim t^{1/2}$ for this class of systems.

(b) *Class 2* systems are those where the minimum energy barriers are again independent of L, but the elementary diffusion process (e.g., a corner moving along an edge) has an energy barrier E_B, so that $a(L,T)=a_0\exp(-E_B/T)$ ($k_B=1$). In this case, we again obtain a $t^{1/2}$-law, but with a time scale $\tau=\tau_0\exp(E_B/T)$. It is evident from the above equation that domain growth will be slow for this class of systems with $L(t)$ constant for times $t\ll\tau$, while for large times the growth law is $L(t)\sim(t/\tau)^{1/2}$.

(c) For *Class 3* systems, the activation energy grows linearly with L. An example of this is a system with quenched impurities that trap the domain walls with a fixed energy (say ϵ) per unit length. In that case, we have a short-time growth law $L(t)\sim t^{1/2}$, which crosses over to a logarithmic growth law at late times, namely, $L(t)\sim T\epsilon^{-1}\ln(t/\tau)$ with $\tau=L_cT/(a_0\epsilon)$, L_c being a crossover length scale.

(d) Finally, *Class 4* systems are those for which the energy barriers grow as L^m, where $m\neq 1$. This situation also

arises in the context of systems with quenched disorder [3]. Again, the short-time growth law is $L(t) \sim t^{1/2}$, which crosses over to a ''logarithmic'' growth law, namely, $L(t) \sim (T\epsilon^{-1})^{1/m}[\ln(t/\tau)]^{1/m}$ with $\tau = L_c^{2-m} T/(m a_0 \epsilon)$, L_c being a crossover length scale.

The general classification described above will prove useful in our subsequent discussion of domain growth in systems with local kinetic barriers.

III. DETAILS OF MODELING

A. Brief review of static properties

The BEG model is a spin-1 Ising model with two order parameters, i.e., the dipole and quadrupole moments, and was initially proposed to study phase separation and superfluid ordering in ^{3}He-^{4}He mixtures [15]. Its subsequent applications include condensation and phase separation in binary and ternary fluids [16], microemulsions [17], semiconducting alloys [18], etc. The BEG model exhibits a rich phase diagram, which has been extensively explored by a variety of techniques [19,20].

In its most general form, the BEG Hamiltonian can be written as follows:

$$H = -J\sum_{\langle ij\rangle} s_i s_j - K\sum_{\langle ij\rangle} s_i^2 s_j^2 - \frac{M}{2}\sum_{\langle ij\rangle} (s_i^2 s_j + s_i s_j^2) - h\sum_i s_i - \Delta\sum_i s_i^2, \quad s_i = \pm 1, 0, \tag{5}$$

where the angular brackets refer to a sum over nearest-neighbor pairs, $J(>0)$ is the ferromagnetic exchange-interaction strength; K is the quadrupole exchange-interaction strength, h is an external magnetic field, and Δ is the anisotropy field. In the present exposition, we focus on the case with $M = h = 0$. Furthermore, our dynamical simulations are in the parameter range $K, \Delta \geqslant 0$.

For our study of far-from-equilibrium dynamics, only broad features of the phase diagram are relevant. Toward this end, it is instructive to examine the nature of the ground state at $T = 0$. There are three possible states—two with equal energy ($s_i = \pm 1 \ \forall i$), and the state $s_i = 0 \ \forall i$. The energy of the two equivalent states is $E_{\pm 1} = -\frac{1}{2}N(qJ + qK + 2\Delta)$, while that of $s_i = 0$ is $E_0 = 0$. Therefore, the ground state is paramagnetic if $(qJ + qK + 2\Delta) < 0$ and ferromagnetic otherwise, and a first-order transition occurs at $\Delta = -(qJ + qK)/2$. For $T > 0$ but small, we expect a similar first-order transition by continuity arguments.

For arbitrary T, we invoke the mean-field (MF) approximation, where it is straightforward to obtain self-consistent equations for the two order parameters, $\langle s_i \rangle \equiv m$ and $\langle s_i^2 \rangle \equiv \rho$. These equations have the form

$$m = \frac{2\sinh(\beta q J m)}{\exp[-\beta(qK\rho + \Delta)] + 2\cosh(\beta q J m)}, \tag{6}$$

$$\rho = \frac{2\cosh(\beta q J m)}{\exp[-\beta(qK\rho + \Delta)] + 2\cosh(\beta q J m)}.$$

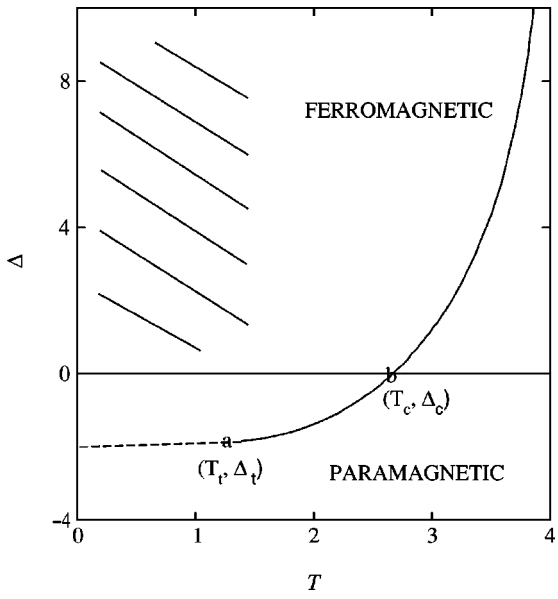

FIG. 1. MF phase diagram of the $d = 2$ BEG model in the (T, Δ) plane when $K, M, h = 0$. Parameters are measured in units of J, i.e., $J = 1$. A line of first-order transitions (dashed line) terminates at the tricritical point (T_t, Δ_t), and continues on as a line of second-order transitions (solid line). The equation of the solid line is $8\beta = \exp(\beta\Delta) + 2$, where $\beta = 1/T$ ($k_B = 1$). Important points marked on the phase diagram are (a) the tricritical point, $(T_t, \Delta_t) = (\frac{4}{3}, -\frac{4}{3}\ln 4)$, and (b) the critical point of the spin-1 Ising model, $(T_c, \Delta_c) = (\frac{8}{3}, 0)$. Our dynamical simulations correspond to quenches from $T = \infty$ to the hatched region of the phase diagram.

In Eq. (6), q is the coordination number and $\beta = 1/T$ with $k_B = 1$. The model reduces to the spin-1 Ising model in the absence of quadrupole and anisotropy terms ($K = \Delta = 0$). This exhibits a second-order paramagnetic-ferromagnetic transition at $T_c = 2q/3$, where we measure quantities in units of J, i.e., $J = 1$. Let us now individually examine the cases $K = 0$ and $\Delta = 0$.

(i) $K = 0$ case. The point $\Delta = -q/2$ corresponds to a first-order transition. As T increases, the transition continues to be first order until a temperature $T_t = q/3$ is reached. The line of first-order transitions terminates at the tricritical point (T_t, Δ_t), where $\Delta_t = -(q/3)\ln(4)$. Beyond this point, the transition is continuous. The relevant MF phase diagram is shown in Fig. 1, and is well-known in the literature [15,19]. Most of our dynamical simulations are in the context of this phase diagram—we consider quenches from a high-temperature disordered phase to the hatched region of the phase diagram. The results presented here for $K = 0$ are quantitatively similar (except for prefactors) to those obtained for $K > 0$, which is the region of interest to us.

(ii) $\Delta = 0$ case. In this case, the first-order transition occurs at $K = -1$. As T increases, we have similar behavior as in the $K = 0$ case, i.e., the transition continues to be first order until a tricritical point is reached. Beyond this point, the transition becomes second order. The detailed MF phase diagram has been explored extensively in Ref. [19].

B. Dynamical version of model

We are interested in investigating the far-from-equilibrium evolution of the BEG model with kinetic constraints. The spin-1 model has no intrinsic dynamical evolution. We introduce stochastic kinetics by placing the system in contact with a heat bath. In this paper, we have used MC simulations to study the BEG model with Glauber spin-flip kinetics on a $d=2$ square lattice. We imposed a kinetic constraint such that transitions from $\pm 1 \rightarrow \mp 1$ were forbidden, i.e., only transitions from $\pm 1 \rightarrow 0$ and $0 \rightarrow \pm 1$ were permitted. Typically, such a kinetic constraint would arise from a selection rule (e.g., quantum-mechanical) governing spin transitions, e.g., $\delta s = \pm 1$. In this paper, we consider physical situations in which $\gamma = \beta\Delta$ is positive and large, so that there is a strong local barrier for the two-step transition $\pm 1 \rightarrow 0 \rightarrow \mp 1$. This mimics a continuous degree of freedom that encounters a barrier while going from one low-energy configuration to another. We would like to understand the implications of this local barrier for phase ordering dynamics in this system.

Before we proceed to describe results, let us briefly present details of our numerical simulation techniques. We have conducted MC simulations of our model with $K, \Delta \geqslant 0$ on lattices of size N^2, with periodic boundary conditions in both directions. Subsequently, we present results for $K=0$ alone, as these are quantitatively similar to results obtained for $K>0$. All parameters are measured in units of J, i.e., $J=1$. We have done simulations with both synchronous and sequential updating, with equivalent results. The results presented in this paper correspond to the case of synchronous updates. The initial condition for a run generally consisted of a random distribution of equal numbers of $+1,0,-1$—corresponding to a high-temperature disordered configuration. At time $t=0$, the system was quenched into the hatched region of the phase diagram in Fig. 1, where the equilibrium state is ferromagnetic. All statistical data presented subsequently is obtained from 5 independent runs with lattice sizes $N=512$, except where stated otherwise. As we demonstrate later, this proved sufficient to obtain high-quality numerical data.

IV. DOMAIN GROWTH AND PATTERN MORPHOLOGY

A. Shrinking of a square droplet

Let us initiate our study of phase ordering in this $d=2$ system by examining a simple situation, i.e., we consider a square droplet of (say) $+1$ in a background of -1. As discussed by Shore *et al.* [6], a careful analysis of this situation clarifies the nature of barriers to the domain growth process, i.e., whether or not the barriers depend upon the length scale.

In this context, a bulk spin-flip (i.e., $+1 \rightarrow 0$) has an energy cost of $(4+4K+\Delta)$. For a boundary (other than corner) spin, the cost is $(2+4K+\Delta)$, and for a corner spin, the cost is $(4K+\Delta)$. Hence, there is always a barrier to evolution when $(4K+\Delta)>0$, and the most probable evolution path in configuration space starts by flipping the corner spin. After the corner spin flips, new corner spins are created and these also have to cross the same energy barrier as their predecessor. This process continues until the last spin in the droplet has been flipped. Therefore, the optimal path for shrinking a square requires surmounting energy barriers of height $E_B = 4K+\Delta$. An increase in L, the square size, increases the number of sites to be flipped but the energy barrier is still the same. This corresponds to a Class 2 system in the LMV classification scheme, discussed in Sec. II.

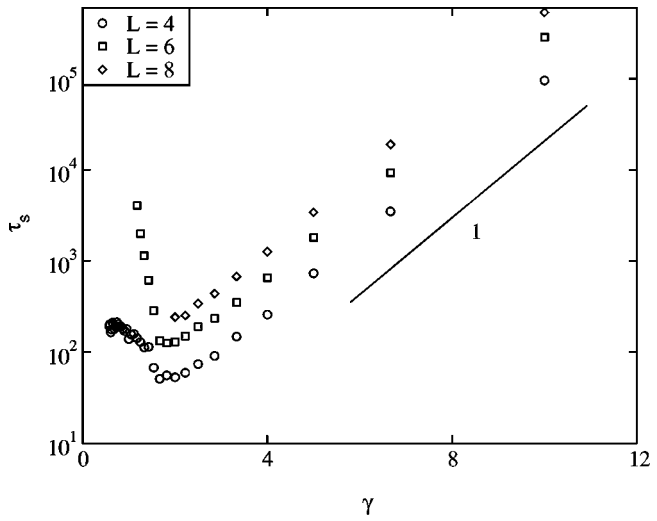

FIG. 2. Barrier dependence of the time to shrink a square droplet (τ_s) in $d=2$ MC simulations. The parameter values were $K=0$, $\Delta=3.2$, and T was varied. We plot τ_s vs $\gamma(=\beta\Delta)$ on a linear-log scale for square droplets of initial sizes $L=4,6,8$ (denoted by the symbols indicated). Each point is obtained as an average over 100 independent runs. The low-T (or high-γ) data corresponds to a straight line with slope 1, confirming that $\tau_s = \tau_0 \exp(\gamma)$ for high γ.

Figure 2 shows MC results for the time to shrink a square droplet (τ_s) in $d=2$, when $K=0$. We present data for τ_s vs $\gamma(=\beta\Delta)$ on a linear-log plot—activation over a constant-energy barrier should yield a straight line with unit slope, i.e., $\tau_s = \tau_0 \exp(\gamma)$. This is seen to be the case for large values of γ in Fig. 2, confirming that there is a constant (rather than length-scale dependent [6]) energy barrier to droplet shrinking.

We can obtain a quantitative estimate of the droplet-shrinking time by using the expression in Eq. (3). At low T, the shrinking process proceeds by the successive removal of layers through the random walk of steps. The shrinking time is obtained as the sum of first-passage times for random walks of size L, $(L-1)$, etc. We are presently investigating this problem in some detail, and quantitative comparisons between theory and numerical simulations will be presented elsewhere.

B. Correlation function and domain-size distribution

Next, let us consider domain growth resulting from an arbitrary initial condition. Figure 3 shows the evolution of an initial condition consisting of a uniformly distributed mix of $+1,0,-1$. The parameter values were $T=0.4$ and $\gamma=8$. Figure 4 shows the corresponding variation of the spin variable $s(i,j)$ along the diagonal $(i=j)$ for the evolution pictures of Fig. 3. At this value of γ, the concentration of 0's rapidly

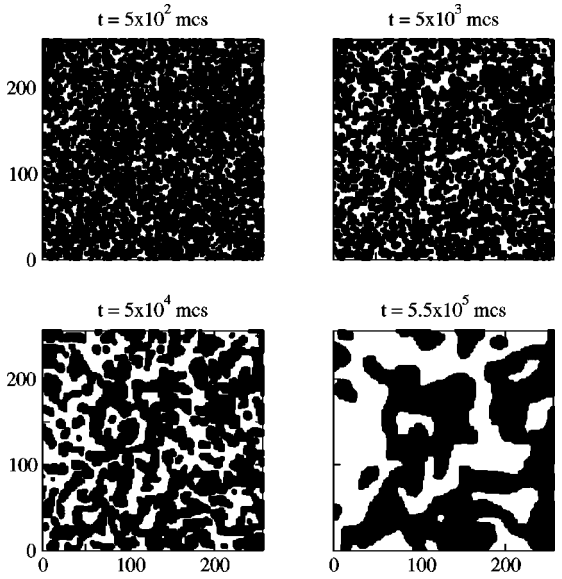

FIG. 3. Evolution pictures for our dynamical model from a random initial condition, consisting of a uniformly distributed mixture of equal amounts of $+1,0,-1$. The parameter values are $T=0.4$ and $\gamma=8$. Typically, most 0's are eliminated in the initial transient regime, and their subsequent density is dictated by the appropriate Boltzmann factor, with a much larger probability of being on the domain boundaries. Our MC simulations were performed on N^2 lattices ($N=512$), with periodic boundary conditions in both directions. For clarity, the snapshots in the figure show only 256^2 segments of the evolving system. In the pictures, $+1$'s are marked in black and -1's are unmarked.

drops to the equilibrium value, and the subsequent morphology consists of coarsening domains rich in either $+1$ or -1. We have confirmed numerically that, after the transient period, the fraction of 0's is determined by the equilibrium Boltzmann factor. Furthermore, the density of 0's is appreciably higher in the interface regions than in the bulk. Based

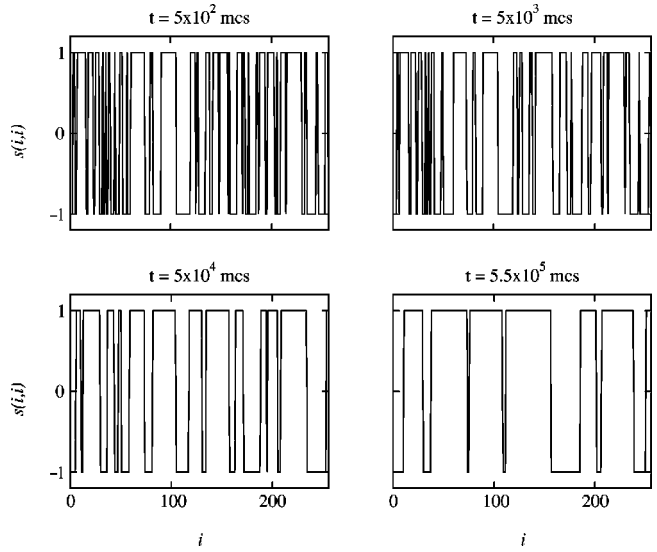

FIG. 4. Variation of the spin variable $s(i,j)$ along the diagonal $(i=j)$ for the snapshots shown in Fig. 3.

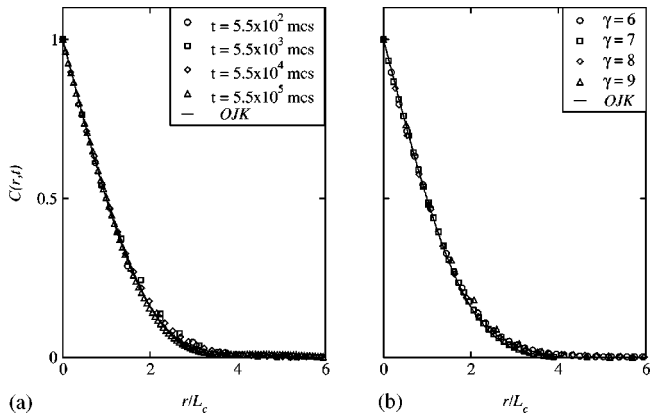

FIG. 5. Dynamical scaling of the spatial correlation function. We plot $C(r,t)$ vs $r/L_c(t)$, where $L_c(t)$ is the distance over which the correlation function falls to half its maximum value. The solid line is the scaled analytic form for spin-1/2 ferromagnets due to (OJK [23], namely, $C(r,t)=(2/\pi)\sin^{-1}(e^{-r^2/t})$. (a) Superposition of data from different times (denoted by the specified symbols) for $T=0.4$ and $\gamma=8$. (b) Superposition of data for $T=0.4$ and different values of $\gamma=6,7,8,9$ (denoted by the specified symbols), at time $t=5.5\times10^4$ mcs.

on our earlier arguments for shrinking of droplets, we expect that domain growth in this case will proceed in the usual fashion for the spin-1/2 Ising model, but with a time scale renormalized by the factor $\exp(\gamma)$.

First, we briefly consider the spatial correlation function and test it for dynamical scaling. As discussed earlier, if scaling holds, we expect the correlation function to have the form $C(\vec{r},t)=g[r/L(t)]$. Figure 5 presents scaled data for the correlation function at (a) different times and $\gamma=8$, and (b) different values of γ. We have followed the usual practice of defining the length scale $L_c(t)$ as the point where the correlation function decays to half its maximum value [1]. The scaled correlation function is in good agreement with the standard result for spin-1/2 ferromagnets due to Ohta *et al.* [23] (OJK), which is depicted as a solid line in Fig. 5.

A more detailed measure of the domain morphology is the domain-size distribution function. This has received considerably less attention in the literature than the real-space correlation function or its Fourier transform, the momentum-space structure factor [1]. In the present paper, we attempt to quantify this distribution function as its functional form will be a useful input in our calculation of the autocorrelation function in Sec. V. Let us denote this distribution function as $P(l,t)$, where domain size $l\in[0,\infty]$, and consider the normalized form such that $\int_0^\infty dlP(l,t)=1$. We have computed $P(l,t)$ numerically by examining the zero crossings of order-parameter profiles of the type shown in Fig. 4. For an individual run, we extract domain-size distributions by sweeping the lattice in both horizontal and vertical directions. Furthermore, as stated earlier, we average data over 5 independent runs.

We now investigate whether the domain distribution function also exhibits dynamical scaling with the form $P(l,t)=L(t)^{-1}f[l/L(t)]$, where $L(t)$ is a measure of the characteristic domain size, e.g., $L(t)=\langle l\rangle$. Figure 6 superposes data

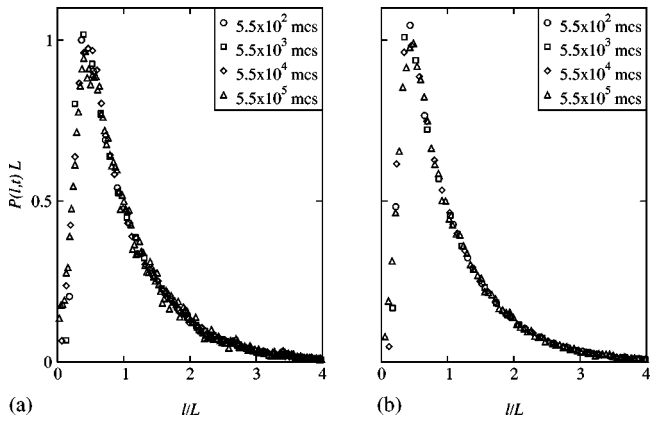

FIG. 6. Domain-size distribution functions for two different values of γ, as specified. We superpose data from different times (denoted by the symbols indicated) for $P(l,t)L(t)$ vs $l/L(t)$, where $L(t)=\langle l\rangle$ is the first moment of $P(l,t)$. The parameter values are $T=0.4$ and (a) $\gamma=8$ and (b) $\gamma=9$. The data sets are obtained from 5 independent runs with $N=512$.

for $P(l,t)L(t)$ vs $l/L(t)$ from different times, confirming the scaling form. Moreover, the scaling functions are numerically indistinguishable for different values of γ, as shown in Fig. 7.

As is evident from Fig. 7(b), the tail of the scaling function exhibits an exponential decay. The entire function can be approximated by the double-exponential form

$$f(x)\simeq a\left[\exp\left(-\frac{2ax}{a+1}\right)-\exp\left(-\frac{2ax}{a-1}\right)\right]$$
$$\equiv a[e^{-b_1x}-e^{-b_2x}], \tag{7}$$

where the function $f(x)$ satisfies $f(0)=0$, $\int_0^\infty dx f(x)=1$, and $\int_0^\infty dx x f(x)=1$.

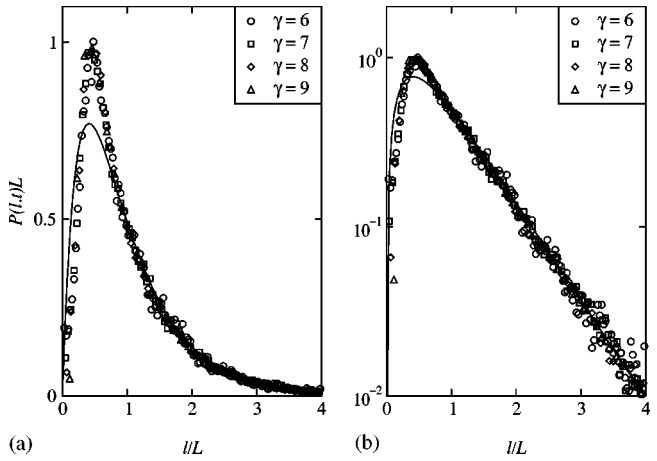

FIG. 7. Scaled domain-size distribution functions for different values of γ at $t=5.5\times10^4$ mcs. We superpose data for $P(l,t)L(t)$ vs $l/L(t)$ for $T=0.4$ and $\gamma=6,7,8,9$ (denoted by the symbols indicated) on (a) a direct plot, and (b) a linear-log plot. The solid line corresponds to the double-exponential function in Eq. (7) with $a\simeq2.0$.

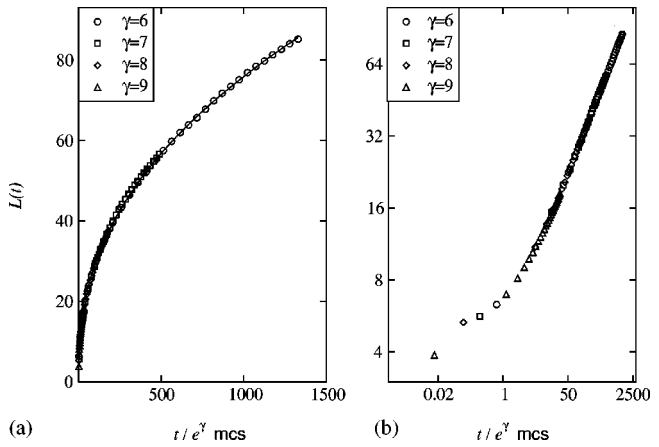

FIG. 8. Time-dependence of characteristic domain length scale. We plot $L(t)$, defined as the first moment of the domain-size distribution function $P(l,t)$, vs t/e^γ on (a) a direct plot, and (b) a log-log plot. We present data for $T=0.4$ and $\gamma=6,7,8,9$—denoted by the specified symbols. The solid line in (a) is a nonlinear fit $L(t)=a+b(t/e^\gamma)^x$ to the data for $\gamma=6$. The best-fit exponent is $x=0.46\pm0.01$, consistent with the Allen-Cahn growth law.

As Fig. 7 demonstrates, the sharp rise to the peak is not captured well by this functional form. We would like to make two remarks in this context. First, the domain sizes below the peak are of the order of 2–3 lattice sites in our simulations. These ''domains'' appear and disappear spontaneously due to thermal fluctuations and are difficult to characterize by a scaling function. Second, one can use more complicated functions to better represent the scaling function. However, as will become clear later, the exponential decay of $f(x)$ subsequent to the peak is the relevant factor, which results in a stretched-exponential form for the autocorrelation function. The double-exponential function provides this feature in a straightforward fashion, besides giving a reasonable description at small x.

Finally, we examine the growth of the characteristic length scale. In the scaling regime, any measure of the length scale exhibits the same dynamical behavior, up to a prefactor. Here, we consider the time dependence of the first moment of the domain-size distribution function, $L(t)$. Figure 8 plots $L(t)$ vs $t/\exp(\gamma)$ for different values of γ. This curve exhibits two distinct regimes. The early-time regime can be identified with the rapid emergence of ±1-domains due to the elimination of 0's, and ends at around $L\simeq4-5$ lattice sites. Following this, domain growth occurs by the random walk of steps along domain boundaries. This results in the AC growth law $L(t)\sim(t/\tau)^{1/2}$, where $\tau=\tau_0\exp(\gamma)$, as we have confirmed from the result in Eq. (3). In discrete systems, this random-walk picture is the counterpart of curvature-driven growth in continuous systems.

The asymptotic regime is in accordance with the behavior of Class 2 systems in the LMV classification. As the temperature $T\to0$, the effective barrier diverges and the dynamics becomes progressively slower. However, the slowing down results from a divergent time scale rather than a functional change in the domain growth law as, for example, in (a) the case with quenched disorder [4,5], or (b) the case of

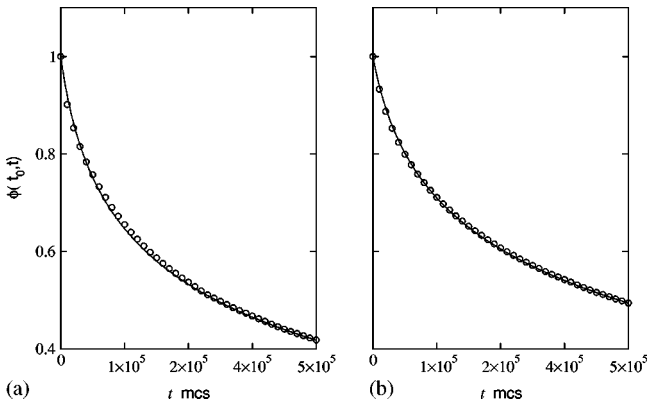

FIG. 9. Plot of the normalized autocorrelation function, $\phi(t_0,t)=\Phi(t_0,t)/\Phi(t_0,0)$ vs t, where $t_0=50\,000$ mcs. We present data for $T=0.4$ and (a) $\gamma=8$, and (b) $\gamma=9$. The solid line is a fit to the analytical form in Eq. (13), with best-fit parameter values $\alpha \simeq 0.05\,(\gamma=8)$, and $\alpha=\simeq 0.06\,(\gamma=9)$.

frustrated nonrandom systems considered by Shore *et al.* [6].

Before we proceed, let us summarize the results of this section. We have demonstrated that local kinetic barriers of the selection-rule type do not add up to give a length-scale dependent barrier. Thus, our system categorizes as Class 2 in the LMV scheme. Domain growth is characterized by divergent time scales as $T\to 0$ and freezes at $T=0$. However, the evolution morphology and the functional form of the domain growth law remain unchanged (except at $T=0$). In particular, we have quantified the domain-size distribution functions, which will be an important input in our study of autocorrelation functions in Sec. V.

V. AUTOCORRELATION FUNCTIONS AND STOCHASTIC MODELING

A. Numerical results and general remarks

Next, we consider the autocorrelation function $\Phi(t_0,t)$ for phase ordering in our model, which is defined as

$$\Phi(t_0,t)=\frac{1}{N^2}\sum_i\,[\langle s_i(t_0)s_i(t_0+t)\rangle-\langle s_i(t_0)\rangle\langle s_i(t_0+t)\rangle], \tag{8}$$

where t_0 is an initial reference time and the angular brackets refer to an average over independent runs with different initial conditions and noise realizations. In the paramagnetic state, each term in the above sum is equal, due to translational invariance. However, this is not true in the low-temperature phase. As we have seen, the evolution proceeds by formation and growth of domains. In this process, spins which are in the domain interiors hardly ever flip, and the time dependence is largely confined to the domain boundaries.

Our numerical results are obtained for a sufficiently large initial time, $t_0=50\,000$ mcs, so that the system is in the asymptotic ordering regime. Figure 9 presents representative results for the autocorrelation function. In Fig. 9, we plot data for $\phi(t_0,t)=\Phi(t_0,t)/\Phi(t_0,0)$ vs t for 2 values of γ. The solid line denotes the best fit to our data using the analytical expression presented later in Eq. (13). This analytical expression (and our numerical results) are consistent with a stretched-exponential behavior at late times, which is a universal feature of systems exhibiting slow dynamics, e.g., structural glasses.

The stretched-exponential behavior of stress relaxation in glasses has been understood in terms of the Glarum model [7]. In this model, localized stresses are relaxed by the diffusion of defects. The multiplicity of relaxation time scales arises due to the range of diffusion times of randomly distributed defects. Another general mechanism for stretched-exponential behavior has been suggested by Ngai *et al.* [8]. In their modeling, relaxation is mediated by quantum modes, e.g., phonons, which have a finite density-of-states at zero energy.

In the specific context of phase ordering systems, there have been some studies of the autocorrelation function. Thus, for the spin-1/2 ferromagnet, an extension of OJK theory (which is a MF result, valid in the limit $d\to\infty$) yields the result [1]

$$\Phi(t_0,t)=\frac{2}{\pi}\sin^{-1}\left[\frac{(1+t/t_0)^{d/4}}{(1+t/2t_0)^{d/2}}\right]. \tag{9}$$

For $t\gg t_0$, we have an approximate power-law decay (rather than stretched exponential), $\Phi(t_0,t)\simeq(4t_0/t)^{d/4}\equiv(4t_0/t)^{\lambda/2}$, where λ is an exponent first introduced by Fisher and Huse [24] in the context of spin glasses. The above result does not account for thermal fluctuations in the system. For example, Huse and Fisher [12] and Tang *et al.* [13] have analytically shown that equilibrium fluctuations in the bulk domains result in a stretched-exponential decorrelation—much faster than the power law obtained from OJK theory. In the context of our dynamical model, we will subsequently provide an understanding of the observed stretched-exponential behavior using a simple stochastic model.

B. Stochastic model for autocorrelation

In this section, we show that the autocorrelation function can be viewed as the correlation function of a dichotomic Markov process in the parameter range of interest to us. We have seen that, at low T and large Δ, the fraction of 0's is very small. The flip of a spin from $\pm 1\to\mp 1$ occurs only via the 0 state, where the spin spends very little time. Thus, the dynamics of domain growth can be viewed in terms of flips between $+1$ and -1 states, with flips at a site mediated by the appearance of 0's.

Let us first focus on a single spin $s_i(t)$, which we model as a dichotomic variable $s_i(t)\in\{-1,+1\}$, with occasional flips that change its value between -1 and $+1$. (We neglect the small fraction of time spent in the 0 state.) We model the occurrence of flips (or appearance of 0's) at the site as a probabilistic Markov process. For this purpose we use the continuous-time random walk (CTRW) formalism [25,26], which has become a powerful tool for describing a range of physical processes like anomalous diffusion, trapping, etc.

[27,28]. The method and its extensions appropriate to the current problem are described in Appendix A. The essential physical input for determination of the autocorrelation function is the so-called waiting-time distribution $\psi(t)$, which is the probability that the spin does not flip in time t if a flip has occurred at $t=0$. The resultant expression for the Laplace transform of the autocorrelation function is [Eq. (A 10) of Appendix A]

$$\Phi(s)=\frac{1}{s}-\frac{2\psi(s)}{\tau_\psi s[2-s\psi(s)]}, \tag{10}$$

where $\psi(s)$ is the Laplace transform of $\psi(t)$, and $\tau_\psi = \int_0^\infty \psi(t)\,dt$. We will now model the waiting-time distribution in the present context.

For large values of γ, the 0's reach an equilibrium density in a short transient time. The probabilities for occurrence of 0's are $p_b \simeq e^{-\beta(4+\Delta)}$ (in the bulk), $p_e \simeq e^{-\beta(2+\Delta)}$ (at an edge), and $p_c \simeq e^{-\beta\Delta}$ (at a corner). The overall fraction of 0's for a domain of size l is $f_l=(p_bV_b+p_eV_e+p_cV_c)/(V_b+V_e+V_c)$, where V_b, V_e, and V_c refer to the volumes of the bulk, edges, and corners, respectively. We expect that $V_b \sim l^2$, $V_e \sim l$, and $V_c \sim l^\theta$, where the exponent θ is zero for smooth interfaces and nonzero for rough interfaces. In equilibrium, interfaces in the $d=2$ Ising model are rough at any $T>0$ [29]. Furthermore, in the nonequilibrium simulations described here, our numerical results show that $\theta \simeq 1$. For our parameter values and time regimes, the dominant contribution to f_l comes from the corners. As length scales increase, the contribution to 0's may arise primarily from the edges or bulk, but we do not access such length scales in our simulations. Thus, the fraction of 0's in the domain is $f_l \simeq g p_c/l$, where g is a geometric factor.

We now assume that the decorrelation process is Poissonian and the flip rate for the autocorrelation function of a domain is proportional to the fraction of 0's. Thus, the corresponding waiting-time distribution is taken as

$$\psi(t)\simeq \exp\left(-\frac{gt}{l\tau}\right), \tag{11}$$

where $\tau=\tau_0 \exp(\gamma)$, with τ_0 being the time scale. Using Eq. (10), we obtain the corresponding autocorrelation function for a domain of size l as

$$\Phi_l(t)\simeq \exp\left(-\frac{2gt}{l\tau}\right), \tag{12}$$

which is the usual exponential decay associated with a Poissonian process. Finally, we introduce the domain morphology through the domain-size distribution function $P(l,t)$, which we had obtained numerically in Sec. IV B. In the NCOP case, correlations between domains are negligible. Assuming that domains evolve independently in time, we have the overall autocorrelation function

$$\begin{aligned}\Phi(t_0,t) &\simeq \int_0^\infty dl\,\Phi_l(t)P(l,t_0+t)\\ &= L(t_0+t)^{-1}\int_0^\infty dl\,\exp\left(-\frac{2gt}{l\tau}\right) f\left(\frac{l}{L(t_0+t)}\right)\\ &\equiv \int_0^\infty dx\,\exp\left[-\frac{\alpha t}{x(t_0+t)^{1/2}e^{\gamma/2}}\right] f(x),\end{aligned} \tag{13}$$

where we have introduced the parameter $\alpha=2g/(b\tau_0^{1/2})$, and $L(t_0+t)\simeq b[(t_0+t)/\tau]^{1/2}$. The fits shown in Fig. 9 were obtained by evaluating the above integral with α as a fitting parameter. The functional form of $f(x)$ was input directly from the numerical simulation results in Fig. 7. The quality of fits shown in Fig. 9 demonstrates that the above arguments capture the basic features of the decorrelation process in our model rather well.

To obtain an analytical understanding of the asymptotic behavior of $\Phi(t_0,t)$, we use the double-exponential form for $f(x)$ from Eq. (7):

$$\begin{aligned}\Phi(t_0,t) &\simeq a\int_0^\infty dx\,\exp\left[-\frac{\alpha t}{x(t_0+t)^{1/2}e^{\gamma/2}}\right](e^{-b_1x}-e^{-b_2x})\\ &\equiv I_1-I_2.\end{aligned} \tag{14}$$

We first focus on the integral I_1. In the asymptotic regime (t large), we perform a saddle-point expansion to obtain

$$I_1\simeq\left(\frac{2\pi a^2}{f''(y_0)}\right)^{1/2}\left[\frac{t^{1/4}}{(t_0+t)^{1/8}e^{\gamma/8}}\right]\exp\left[-\frac{f(y_0)t^{1/2}}{(t_0+t)^{1/4}e^{\gamma/4}}\right], \tag{15}$$

where

$$\begin{aligned}f(y)&=\frac{\alpha}{y}+b_1y,\\ y_0&=\left(\frac{\alpha}{b_1}\right)^{1/2}.\end{aligned} \tag{16}$$

A similar expression is obtained for I_2 in the saddle-point approximation when t is large. The asymptotic form for the autocorrelation function is a stretched exponential, with the stretching exponent $\beta=1/4$ in this regime. The (slow) stretched-exponential decay results from the convolution of exponential decays of individual domains with the domain-size distribution function. For much later times, the primary contribution to f_l is from the bulk domains. In that regime, our simple arguments above result in an exponential decay for the autocorrelation function.

A more accurate calculation of decorrelations arising from spins in domain interiors involves two waiting-time distributions, and is outlined in Appendix A. However, as we said earlier, the parameter values used here effectively eliminate decorrelations arising from bulk fluctuations. Therefore, for the sake of brevity, we will not describe the requisite calculation here.

VI. SUMMARY AND CONCLUSION

Let us conclude this paper with a brief summary and discussion of our results. We have undertaken a comprehensive MC simulation of a spin-1 model with constrained dynamics. The constraint has the form of a selection rule $\delta s = \pm 1$ so that $\pm 1 \to 0$ and $0 \to \pm 1$ are the only transitions permitted. Additionally, the state $s=0$ has an appreciably higher energy than the states $s=\pm 1$, giving rise to local kinetic barriers. We have investigated far-from-equilibrium dynamics in this model—resulting from a rapid quench from a high-temperature disordered (paramagnetic) state to a low-temperature state, where the system prefers to be ordered (ferromagnetic).

We have studied two aspects of domain growth in this problem. First, we considered the domain morphology and its evolution, as characterized by the spatial correlation function, the domain-size distribution function, and the time-dependence of characteristic length scales. Our results demonstrate that local barriers do not add up cooperatively to give length-scale dependent barriers. The temporal evolution is analogous to that for the usual spin-1/2 ferromagnet, with time scales renormalized by the Boltzmann factor resulting from the local barrier. Thus, our system is a Class 2 system in the LMV classification scheme [22]. A feature of our present paper is a careful characterization of the domain-size distribution function, which is an important input in the second part of our paper.

The second aspect of domain growth investigated by us is the dynamical behavior of the autocorrelation function. We have formulated a simple stochastic model based on dichotomic Markov processes to mimic spin dynamics in our model. Our analytical results predict a stretched-exponential behavior over an extended time regime, which is consistent with our numerical results. A similar behavior has also been predicted in the context of equilibrium fluctuations in the ordered state of ferromagnets by Huse and Fisher [12] and Tang *et al.* [13]. Clearly, the Huse-Fisher argument also applies to bulk domains in the nonequilibrium evolution considered here, but these effects have been neglected in the present discussion. It is straightforward to incorporate the bulk decorrelations in the framework presented here. Of course, the resulting contributions to the autocorrelation function are translationally invariant in time, unlike the decorrelations arising at the moving interfaces.

At present, we are investigating constrained kinetics in systems with conserved order parameters, e.g., vacancy-mediated phase separation in binary alloys [30]. In that case, local barriers of the type discussed here are not relevant. Nevertheless, a range of interesting behaviors is seen in the COP context also, as we will report in detail at a later stage.

ACKNOWLEDGMENTS

We thank M. Barma, S. P. Das, and J. D. Shore for useful discussions. We also thank J. D. Shore for sending us a copy of his Ph.D. thesis. We are grateful to R. Ramaswamy and the Bio-Informatics Center of Jawaharlal Nehru University for permitting usage of their computational facilities during the preliminary investigation of the problems discussed here. K.T. is also grateful to S. K. Das and R. Mehrotra for their help in debugging program codes.

APPENDIX A: CONTINUOUS-TIME RANDOM WALKS

In this appendix, we present relevant details of the standard continuous-time random walk CTRW formalism. In this method, one introduces the probability $p(n,t)$ that exactly n flips of a spin $s(t) \in \{-1,+1\}$ occur in time t. For the stochastic variable $s(t)$, whose value at $t=0$ is s_0, the probability $p(s,t|s_0)$ of finding the value s at time t is

$$p(s,t|s_0) = \delta_{s,s_0} \sum_{n \text{ even}} p(n,t) + \delta_{s,-s_0} \sum_{n \text{ odd}} p(n,t). \tag{A1}$$

The autocorrelation function $\Phi(t)$ of this stochastic process is given by

$$\Phi(t) = \sum_{s=\pm 1} \sum_{s_0=\pm 1} s s_0 p(s,t|s_0) w(s_0), \tag{A2}$$

where $w(s_0)$ is the initial-state distribution function for the stochastic variable. Thus,

$$\begin{aligned} \Phi(t) &= \left[\sum_{n \text{ even}} p(n,t) - \sum_{n \text{ odd}} p(n,t) \right] \sum_{s_0=\pm 1} s_0^2 w(s_0) \\ &\equiv \sum_{n \text{ even}} p(n,t) - \sum_{n \text{ odd}} p(n,t), \end{aligned} \tag{A3}$$

because $s_0^2 = 1$.

The CTRW method computes the probabilities $p(n,t)$ in terms of the so-called waiting-time distribution function $\psi(t)$, which has a central role in the physical formulation of the process. The function $\psi(t)$ is the probability that the spin does not flip in time t, if a flip has occurred at $t=0$. In terms of $\psi(t)$ and its time-derivative $\dot{\psi}(t)$, we can obtain an expression for $p(n,t)$:

$$\begin{aligned} p(n,t) &= \int_0^t dt_n \int_0^{t_n} dt_{n-1} \cdots \int_0^{t_2} dt_1 \psi(t-t_n) \\ &\quad \times [-\dot{\psi}(t_n - t_{n-1})][-\dot{\psi}(t_{n-1}-t_{n-2})] \cdots \\ &\quad \times [-\dot{\psi}(t_2 - t_1)][-\dot{\psi}_0(t_1)] \\ &= (-1)^n \int_0^t dt_n \int_0^{t_n} dt_{n-1} \cdots \int_0^{t_2} dt_1 \psi(t-t_n) \\ &\quad \times \dot{\psi}(t_n - t_{n-1}) \dot{\psi}(t_{n-1}-t_{n-2}) \cdots \dot{\psi}(t_2 - t_1) \dot{\psi}_0(t_1). \end{aligned} \tag{A4}$$

Here, $\psi_0(t)$ represents the waiting-time distribution for the first flip, which is given in terms of $\psi(t)$ by the relation

$$\psi_0(t) = \frac{1}{\tau_\psi} \int_t^\infty dt' \psi(t'), \tag{A5}$$

where $\tau_\psi = \int_0^\infty \psi(t)dt$.

Next, we consider the generating function $H(z,t)$, defined as

$$H(z,t) = \sum_{n=0}^{\infty} z^n p(n,t). \tag{A6}$$

Its Laplace transform,

$$H(z,s) = \int_0^\infty dt e^{-st} H(z,t), \quad \mathrm{Re}(s) > 0, \tag{A7}$$

is determined in terms of the Laplace transform $\psi(s)$ as

$$H(z,s) = \frac{1}{s} + \frac{(z-1)\psi(s)}{\tau_\psi s[1 - z + zs\psi(s)]}. \tag{A8}$$

Returning to the computation of the autocorrelation function, we note that its Laplace transform is given by

$$\Phi(s) = \int_0^\infty dt e^{-st} \Phi(t) = \sum_{n\ \mathrm{even}} p(n,s) - \sum_{n\ \mathrm{odd}} p(n,s). \tag{A9}$$

This quantity can be directly obtained by setting $z = -1$ in $H(z,s)$, yielding the compact expression:

$$\Phi(s) = \frac{1}{s} - \frac{2\psi(s)}{\tau_\psi s[2 - s\psi(s)]}. \tag{A10}$$

The above discussion is valid for spins with flip probability independent of the state, e.g., corner spins with equal numbers of -1 and +1 neighbors. For spins inside bulk domains, it is useful to consider the following generalization of the above treatment. We introduce two waiting-time distributions due to the fact that, in (say) an up domain, the time for flipping from up to down is much longer than from down to up. For an up domain, let $\psi(t)$ and $\phi(t)$ be the waiting times for a spin-flip from ''up to down'' and ''down to up,'' respectively. [For the down domain, the roles of $\psi(t)$ and $\phi(t)$ are reversed.] We can write the probabilities for n flips in an up domain as follows:

$$p(0,t) = \psi_0(t),$$

$$p(1,t) = \int_0^t dt_1 \phi(t - t_1)[-\dot{\psi}_0(t_1)],$$

$$p(2,t) = \int_0^t dt_2 \int_0^{t_2} dt_1 \psi(t - t_2)[-\dot{\phi}(t_2 - t_1)][-\dot{\psi}_0(t_1)],$$

$$p(3,t) = \int_0^t dt_3 \int_0^{t_3} dt_2 \int_0^{t_2} dt_1 \phi(t - t_3)[-\dot{\psi}(t_3 - t_2)] \times [-\dot{\phi}(t_2 - t_1)][-\dot{\psi}_0(t_1)], \tag{A11}$$

and so on. From this, the relevant Laplace transforms are obtained as follows:

$$\sum_{n\ \mathrm{even}} p(n,s) = \psi_0(s) + \psi(s)\dot{\phi}(s)\dot{\psi}_0(s) + \psi(s)\dot{\phi}(s)\dot{\psi}(s)\dot{\phi}(s)\dot{\psi}_0(s) + \cdots = \psi_0(s) + \psi(s)\frac{1}{1 - \dot{\phi}(s)\dot{\psi}(s)}\dot{\phi}(s)\dot{\psi}_0(s),$$

$$\sum_{n\ \mathrm{odd}} p(n,s) = -\phi(s)\dot{\psi}_0(s) - \phi(s)\dot{\psi}(s)\dot{\phi}(s)\dot{\psi}_0(s) - \cdots = -\phi(s)\frac{1}{1 - \dot{\phi}(s)\dot{\psi}(s)}\dot{\psi}_0(s). \tag{A12}$$

Substituting the above results in the expression for the autocorrelation function, one obtains the expression

$$\Phi(s) = \frac{1}{s} - \frac{1}{\tau_\psi s}\frac{2\phi(s)\psi(s)}{\phi(s) + \psi(s) - s\phi(s)\psi(s)}, \tag{A13}$$

where $\tau_\psi = \int_0^\infty dt \psi(t)$. Note that, if $\phi(s) = \psi(s)$, $\Phi(s)$ reduces to our earlier expression in Eq. (A10).

[1] For reviews, see K. Binder, in *Materials Science and Technology, Vol. 5 : Phase Transformations in Materials*, edited by R.W. Cahn, P. Haasen and E.J. Kramer (VCH, Weinheim, New York, 1991) p. 405; A.J. Bray, Adv. Phys. **43**, 357 (1994).

[2] K. Binder and D. Stauffer, Phys. Rev. Lett. **33**, 1006 (1974).

[3] D.A. Huse and C.L. Henley, Phys. Rev. Lett. **54**, 2708 (1985).

[4] For Monte Carlo (MC) studies with quenched disorder, see G.S. Grest and D.J. Srolovitz, Phys. Rev. B **32**, 3014 (1985); D. Chowdhury, M. Grant, and J.D. Gunton, *ibid.* **35**, 6792 (1987); A.J. Bray and K. Humayun, J. Phys. A **24**, L1185 (1991).

[5] For coarsegrained studies with quenched disorder, see S. Puri, D. Chowdhury, and N. Parekh, J. Phys. A **24**, L1087 (1991); S. Puri and N. Parekh, *ibid.* **25**, 4127 (1992); M.F. Gyure, S.T. Harrington, R. Strilka, and H.E. Stanley, Phys. Rev. E **52**, 4632 (1995).

[6] J.D. Shore and J.P. Sethna, Phys. Rev. B **43**, 3782 (1991); J.D. Shore, M. Holzer, and J.P. Sethna, *ibid.* **46**, 11 376 (1992); J.D. Shore, thesis, Cornell University, 1992.

[7] S.H. Glarum, J. Chem. Phys. **33**, 639 (1960).

[8] K.L. Ngai, Comments Solid State Phys. **9**, 127 (1979); K.L. Ngai and A.K. Rajagopal, in *Non-Debye Relaxation in Condensed Matter Physics*, edited by T.V. Ramakrishnan and M.R. Lakshmi (World Scientific, Singapore, 1987).

[9] A.T. Ogielski, Phys. Rev. B **32**, 7384 (1985).

[10] J. Jäckle, Rep. Prog. Phys. **49**, 171 (1986), and references therein.

[11] S. Franz, S.C. Glotzer, and S. Sastry, J. Phys.: Condens. Matter **12**, 29 (2000).
[12] D.A. Huse and D.S. Fisher, Phys. Rev. B **35**, 6841 (1987).
[13] C. Tang, H. Nakanishi, and J.S. Langer, Phys. Rev. A **40**, 995 (1989).
[14] I.S. Graham and M. Grant, J. Phys. A **25**, L1195 (1992).
[15] M. Blume, V.J. Emery, and R.B. Griffiths, Phys. Rev. A **4**, 1071 (1971).
[16] J. Lajzerowicz and J. Sivardiere, Phys. Rev. A **11**, 2079 (1975); J. Sivardiere and J. Lajzerowicz, *ibid.* **11**, 2090 (1975); **11**, 2101 (1975).
[17] M. Schick and W.-H. Shih, Phys. Rev. B **34**, 1797 (1986).
[18] J. Ni and S. Iwata, Phys. Rev. B **52**, 3214 (1995).
[19] For mean-field approaches, see D. Furman, S. Dattagupta, and R.B. Griffiths, Phys. Rev. B **15**, 441 (1977); W. Hoston and A.N. Berker, Phys. Rev. Lett. **67**, 1027 (1991).
[20] For renormalization-group approaches, see T.W. Burkhardt, Phys. Rev. B **14**, 1196 (1970); M. Kaufman, R.B. Griffiths, J.M. Yeomans, and M.E. Fisher, Phys. Rev. B **23**, 3448 (1991).
[21] The formula due to Lagrange is quoted in W. Feller, *Introduction to Probability Theory and its Applications* (Wiley, New York, 1968) p. 353.
[22] Z.W. Lai, G.F. Mazenko, and O.T. Valls, Phys. Rev. B **37**, 9481 (1988).
[23] T. Ohta, D. Jasnow, and K. Kawasaki, Phys. Rev. Lett. **49**, 1223 (1982).
[24] D.S. Fisher and D.A. Huse, Phys. Rev. B **38**, 373 (1988).
[25] E.W. Montroll and G.H. Weiss, J. Math. Phys. **6**, 167 (1965); E.W. Montroll and H. Scher, J. Stat. Phys. **9**, 101 (1973).
[26] J.T. Bendler and M.F. Shlesinger, in *The Wonderful World of Stochastics*, edited by M.F. Shlesinger and G.H. Weiss (Elsevier, Amsterdam, 1985) p. 32.
[27] J. Klafter and R. Silbey, J. Chem. Phys. **72**, 843 (1980).
[28] H. Schnörer and A. Blumen, Phys. Rev. A **41**, 5702 (1990).
[29] D.J. Wallace and R.K.P. Zia, Phys. Rev. Lett. **43**, 808 (1979); J.D. Weeks, in *Ordering in Strongly Fluctuating Condensed Matter Systems*, edited by T. Riste (Plenum, New York, 1980); and references therein.
[30] S. Puri, Phys. Rev. E **55**, 1752 (1997); S. Puri and R. Sharma, *ibid.* **57**, 1873 (1998).